

High-temperature continuous wave operation of strain-balanced quantum cascade lasers grown by metal organic vapor-phase epitaxy

L. Diehl^{a)}*Division of Engineering and Applied Sciences, Harvard University, Cambridge, Massachusetts 02138*

D. Bour, S. Corzine, J. Zhu, and G. Höfler

*Agilent Laboratories, 3500 Deer Creek Road, Palo Alto, California 94304*M. Lončar, M. Troccoli, and Federico Capasso^{b)}*Division of Engineering and Applied Sciences, Harvard University, Cambridge, Massachusetts 02138*

(Received 18 April 2006; accepted 28 June 2006; published online 21 August 2006)

The authors report the fabrication of high-power strained quantum cascade lasers working in continuous mode above 370 K. The devices, processed in narrow buried heterostructures, were grown by low-pressure metal organic vapor-phase epitaxy. Continuous wave output power as high as 312 mW at 300 K was obtained at a wavelength of 5.29 μm from a 3.25 mm long, 7.5 μm wide laser with a high-reflectivity back facet coating. The slope efficiency was in excess of 1.5 W/A and the power conversion efficiency reached almost 5%. © 2006 American Institute of Physics.

[DOI: 10.1063/1.2337284]

In the past few years, the performance of quantum cascade lasers¹ (QCLs) grown by molecular beam epitaxy (MBE) has improved tremendously and high-power continuous wave (cw) operation at room temperature has been since routinely achieved at various wavelengths.^{2,3} Short-wavelength (5.25 μm) QCLs with a maximum cw output power of 480 mW were reported in Ref. 4. This result was obtained at room temperature (298 K) with a strained QC structure based on a double-phonon resonance¹ processed into 11 μm wide ridge waveguide. Together with the large cw output power achievable by QCLs at room temperature, the wavelength range accessible to these devices makes them very attractive, in particular, for compact gas sensors based on photoacoustic spectroscopy.⁵

Metal organic vapor-phase epitaxy (MOVPE) is a widely established platform for the high-volume production of low cost and reliable semiconductor lasers. This technique allows the deposition of uniform and thick layers at high rates. It offers also excellent stability over long growth runs and short machine downtime. MOVPE is thus particularly well suited for the industrial production of QCLs. Recent work showed that the performance obtained with lattice-matched and strained QCLs deposited by MOVPE is comparable with that of similar structures grown by MBE.^{6–8} Recently, we demonstrated high-power ($\cong 200$ mW) cw operation at room temperature of $\lambda \cong 8.38$ μm lattice-matched QCLs grown by MOVPE.⁹

In the present letter, we report the cw operation of strained QCLs at temperatures ranging from 300 to 385 K. The devices studied were processed into buried heterostructures and a high-reflectivity (HR) coating was evaporated on the back facet. With a 7.5 μm wide 3.25 mm long back facet coated laser, we measured low threshold current densities at room temperature equal to 1.23 kA/cm² in pulsed mode and to 1.53 kA/cm² in cw, together with high cw output power in excess of 300 mW at 300 K. The maximum operating tem-

perature was as high as 376 K for this particular device. This represents a major improvement compared to our previous results obtained with similar devices, which operated only up to approximately 280 K in cw mode.⁸

The QCL structure studied in the present work was deposited on a heavily doped *n*-type ($n \approx 3 \times 10^{18}$ cm³) InP substrate by low-pressure (76 Torr) MOVPE without growth interruption at the barrier/quantum well interfaces. The growth conditions were similar to the ones described in Refs. 7–9. The deposition rate was 0.5 nm/s throughout the structure, except for the active region, which was grown at a slower rate of 0.1 nm/s. The cladding layers consist of a 3.5 μm thick InP layer doped with silicon ($n \approx 1 \times 10^{17}$ cm³). The lower cladding layer helps in decoupling the optical mode from the heavily doped substrate, preventing substantial free-carrier absorption. The waveguide core is composed of two 0.33 μm thick *n*-doped ($n \approx 3 \times 10^{16}$ cm³) InGaAs layers and the active region. The latter comprises 30 stages and is based on a double-phonon resonance design identical, except for the doping level in the injector, to the one reported by Hofstetter *et al.*¹⁰ The growth ended with a 0.5 μm thick InP plasmon-enhanced confinement¹ layer doped with silicon ($n \approx 5 \times 10^{18}$ cm³), followed by two heavily doped contact layers (10 nm, *n*+ InP/20 nm, *n*+ InGaAs). Overall, the structure described above is very similar to the double-phonon laser reported in a previous article.⁸ The main difference resides in the doping level being lowered by a factor of 2 in all of the doped layers comprising the claddings and waveguide core (including the active region).

The grown structure was processed into buried heterostructure lasers. Ridges 3 and 7.5 μm wide were defined by conventional photolithography techniques and etched down to approximately half of the lower cladding layer by reactive ion etching. Using MOVPE, InP doped with Fe was then selectively regrown around the ridges to enhance the lateral heat dissipation from the active region. The level of Fe doping was chosen to slightly exceed the background doping of the MOVPE reactor. Since Fe atoms introduced in InP act as

^{a)}Electronic mail: ldiehl@deas.harvard.edu^{b)}Electronic mail: capasso@deas.harvard.edu

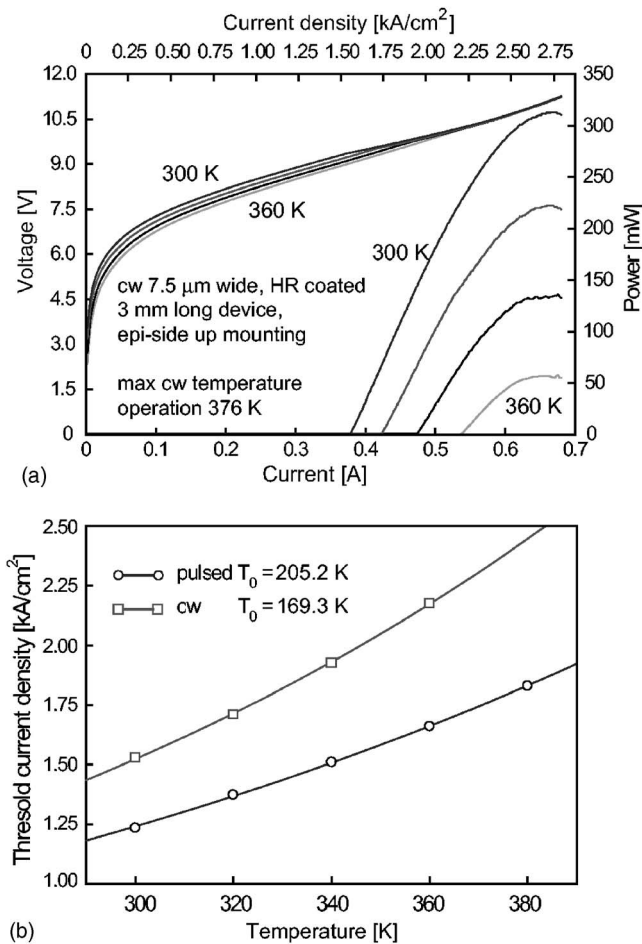


FIG. 1. (a) V - I / L - I curves obtained at different temperatures in cw mode with a $7.5 \mu\text{m}$ wide, 3.25 mm long HR-coated device. (b) Threshold current density measured in pulsed and cw modes vs temperature. The experimental points were fitted with the empirical relation $j_{\text{th}} = j_0 \exp(T/T_0)$.

deep carrier traps, there are essentially no free electrons in the regrown InP layer, resulting in insulating and optically transparent regions around the laser ridges. The next fabrication steps include the evaporation of Ti/Au top contacts followed by the electroplating of a $5 \mu\text{m}$ thick Au layer. Thinning of the substrate and the deposition of a Ge/Au back contact finished the processing. The devices were subsequently cleaved into cavities of different lengths before being soldered episcide up onto Cu heat sinks. A HR coating consisting of $\text{Al}_2\text{O}_3/\text{Au}$ ($200/30 \text{ nm}$) layers was evaporated on the back facet of the QCLs. The voltage and output power versus current (V - I / L - I) characteristics were obtained with the devices placed into a box equipped with thermoelectric cooler. The output power was measured using a polished metallic pipe guiding the light from the laser front facet directly onto the surface of a calibrated thermopile detector. The collection efficiency of this setup is considered to be near 100%. The spectral characterization was performed with a Fourier transform infrared spectrometer equipped with a deuterated triglycine sulphate detector.

The V - I / L - I curves obtained in continuous mode from a 3.25 mm long, $7.5 \mu\text{m}$ wide and HR-coated QCLs are shown in Fig. 1(a). The cw threshold current density j_{th} for this device was 1.53 kA/cm^2 at room temperature and the corresponding slope efficiency was 1.570 W/A . The largest output powers obtained at 300 and 360 K were 312 and 57 mW, respectively. The highest cw temperature operation

T_{max} was 376 K and by reducing the temperature to 260 K, more than 500 mW of cw output power was achieved. The maximum wall-plug efficiency, defined as the total optical power divided by the electrical power, reached 4.6% at 300 K. This device has performance comparable to the best and most recent results obtained with slightly broader MBE-grown QCLs emitting at the same wavelength.⁴

Figure 1(b) is a plot of the threshold current densities obtained at various heat sink temperatures from the HR-coated device described in the previous paragraph. These data were deduced from the cw measurements presented in Fig. 1(a) and from measurements obtained in pulsed mode. In the latter case, the repetition rate was 80 kHz and the pulse width was 125 ns. From these data, high characteristic temperatures T_0 equal to 205.2 K in pulsed mode and 169.3 K in cw mode were deduced. T_0 describes empirically the increase in threshold current versus temperature according to an exponential function $j_{\text{th}}(T) = j_0 \exp(T/T_0)$. The thermal resistance of the device R_{th} can also be calculated from the measurements presented in Fig. 1(b) and yields 12.14 K/W at 300 K.¹¹ It corresponds to a thermal conductance $G_{\text{th}} = 1/(AR_{\text{th}}) = 337.9 \text{ W/(K cm}^2)$, where A is the device area. Using the value found for R_{th} , the temperature difference ΔT between the heat sink and the active region reaches at 300 K $\Delta T = R_{\text{th}} P_{\text{elec}} = 42.8 \text{ K}$. Here P_{elec} is the electrical power dissipated in the device.

Figures 2(a) and 2(b) show data qualitatively similar to those displayed in Fig. 1. This second set of measurements was, however, obtained from a $3 \mu\text{m}$ wide laser. The other device characteristics such as the cavity length were otherwise identical. The cw output power was as high as 97 mW at 300 K, which is noteworthy given the narrow width of this QCL. The corresponding slope efficiency was 1.19 W/A . The threshold current densities measured at room temperature were 1.39 and 1.43 kA/cm^2 in pulsed and cw modes, respectively. The value of j_{th} in pulsed mode is only slightly larger than the one obtained with the $7.5 \mu\text{m}$ wide structure. This is consistent with the results of two-dimensional mode profile simulations, which showed that the mode overlap factor Γ is comparable for both the narrow and broad samples (53.3% and 61.6%, respectively). The inset of Fig. 3 shows a typical spectrum obtained at a current 5% above threshold with the narrow QCL. Note that when the devices studied are pumped 30% or more above j_{th} , the optical spectrum broadens and is composed by many neighboring longitudinal modes. A detailed study of this phenomenon will be given elsewhere. The emission wavelength is $5.29 \mu\text{m}$ and is very close to the designed value.¹⁰

The thermal resistance for the narrowest QCL is 7.01 K/W , which translates into $G_{\text{th}} = 1461 \text{ W/K cm}^2$. This value is comparable to the one found for state-of-the-art buried heterostructure QCLs whose performance was reported in Ref. 12. The ratio of the thermal conductance found for the broad and narrow samples does not match the ratio of the lasers widths. However, it indicates clearly that lateral heat transfer is a major factor in the thermal resistance of the device. This is also in agreement with the fact that the quantity T_0 has a comparable value in pulsed and cw modes for the narrow device (pulsed mode, $T_0 = 189.3 \text{ K}$; cw mode, $T_0 = 185.7 \text{ K}$), while T_0 in the case of the $7.5 \mu\text{m}$ QCL decreases by almost 35 K (pulsed mode, $T_0 = 205.2 \text{ K}$; cw mode, $T_0 = 169.3 \text{ K}$).

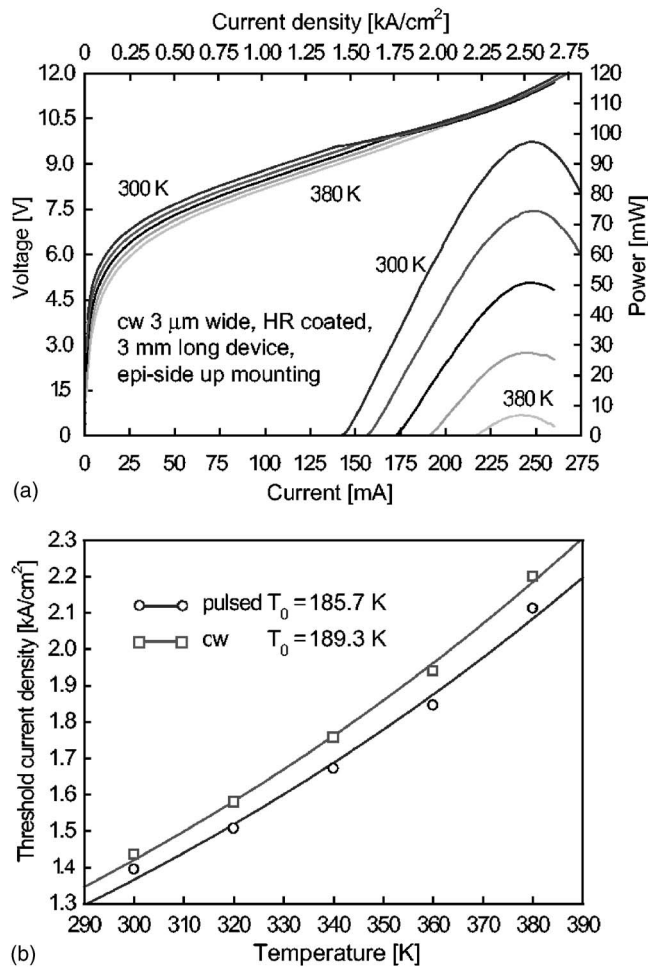


FIG. 2. (a) V - I - L - I curves obtained at different temperatures in cw mode with a $3\ \mu\text{m}$ wide, $3.25\ \text{mm}$ long HR-coated device. (b) Threshold current density measured in pulsed and cw modes vs temperature. The experimental points were fitted with the empirical relation $j_{\text{th}} = j_0 \exp(T/T_0)$.

Three μm wide, HR-coated devices with different cavity lengths were also measured. The longest sample ($4.25\ \text{mm}$) had the highest cw operating temperature ($385\ \text{K}$) and the largest output power, which reached $136\ \text{mW}$ at $300\ \text{K}$. The threshold current density measured in pulsed mode for 1.09 , 1.75 , 2.25 , 3.25 , and $4.25\ \text{mm}$ long cavity is reported in Fig. 3 as a function of the inverse of the cavity length. From these data, the waveguide losses α_w were deduced assuming that the gain cross section does not depend on the current density.¹³ The value of α_w calculated from the fit of the experimental points is only $3.8\ \text{cm}^{-1}$, which compares well with the numbers reported in Ref.¹⁴

In summary, we have presented the high-power cw operation at high temperature of $5.29\ \mu\text{m}$ wavelength strained QCLs grown by low-pressure MOVPE. The characteristics of our lasers are comparable to the best and most recent results obtained from MBE-grown material. Our devices have the highest operating cw temperature reported so far for QCLs at this wavelength. The present work demonstrates that MOVPE meets all the requirements necessary to grow

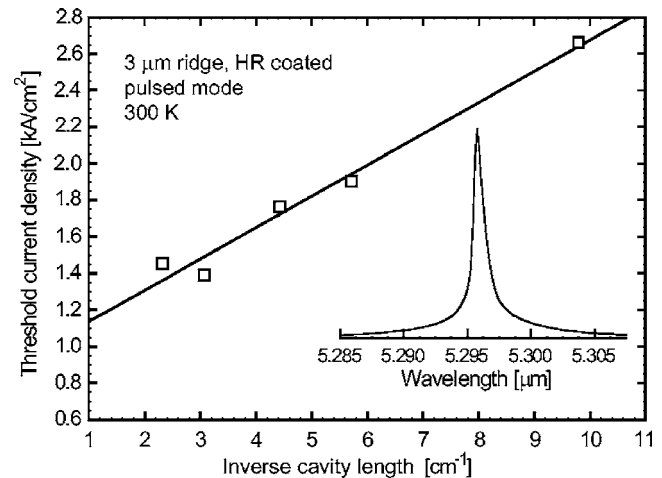


FIG. 3. Pulsed threshold current density and device thermal resistance measured at $300\ \text{K}$ with $3\ \mu\text{m}$ wide HR-coated lasers having a different cavity length. The inset shows an optical spectrum measured with the $3\ \mu\text{m}$ wide, $3.25\ \text{mm}$ long HR-coated device operated in cw mode close to threshold.

high-performance state-of-the-art QCLs, even with demanding material constraints such as large strain.

The Harvard group acknowledges partial financial support from Agilent Technologies, from the U.S. Army Research Laboratory and the U.S. Army Research Office under Grant No. W911NF-04-1-0253, and from DARPA (Optofluidics Center) under Grant No. HR0011-04-1-0032. The Center for Nanoscale Systems (CNS) at Harvard University is also gratefully acknowledged. Harvard-CNS is a member of the National Nanotechnology Infrastructure Network (NNIN).

- ¹F. Capasso, C. Gmachl, D. L. Sivco, and A. Y. Cho, *Phys. Today* **55**(5), 34 (2002).
- ²J. S. Yu, S. Slivken, A. Evans, S. R. Darvish, J. Nguyen, and M. Razeghi, *Appl. Phys. Lett.* **88**, 091113 (2006).
- ³J. S. Yu, S. Slivken, A. Evans, S. R. Darvish, J. Nguyen, and M. Razeghi, *Appl. Phys. Lett.* **88**, 091113 (2006).
- ⁴A. Evans, J. Nguyen, S. Slivken, J. S. Yu, S. R. Darvish, and M. Razeghi, *Appl. Phys. Lett.* **88**, 51105 (2006).
- ⁵A. Kosterev and F. Tittel, *IEEE J. Quantum Electron.* **38**, 582 (2002).
- ⁶R. P. Green, L. R. Wilson, E. A. Zibik, D. G. Revin, J. W. Cockburn, C. Pflügl, W. Schrenk, G. Strasser, A. B. Krysa, J. S. Roberts, C. M. Tey, and A. G. Cullis, *Appl. Phys. Lett.* **85**, 5529 (2004).
- ⁷M. Troccoli, S. Corzine, D. Bour, J. Zhu, O. Assayag, L. Diehl, B. G. Lee, G. Höfler, and F. Capasso, *Electron. Lett.* **41**, 1059 (2005).
- ⁸L. Diehl, D. Bour, S. Corzine, J. Zhu, G. Höfler, B. G. Lee, C. Y. Wang, M. Troccoli, and F. Capasso, *Appl. Phys. Lett.* **88**, 041102 (2006).
- ⁹L. Diehl, D. Bour, S. Corzine, J. Zhu, G. Höfler, M. Lončar, M. Troccoli, and F. Capasso, *Appl. Phys. Lett.* **88**, 201115 (2006).
- ¹⁰D. Hofstetter, M. Beck, T. Aellen, and J. Faist, *Appl. Phys. Lett.* **78**, 396 (2001).
- ¹¹S. Blaser, D. A. Yarekha, L. Hvozdar, Y. Bonetti, A. Müller, M. Giovannini, and J. Faist, *Appl. Phys. Lett.* **86**, 41109 (2005).
- ¹²A. Evans, J. S. Yu, J. David, L. Doris, K. Mi, S. Slivken, and M. Razeghi, *Appl. Phys. Lett.* **84**, 314 (2004).
- ¹³C. Sirtori, J. Faist, F. Capasso, D. Sivco, A. Hutchinson, and A. Cho, *Appl. Phys. Lett.* **66**, 3242 (1995).
- ¹⁴T. Gresch, M. Giovannini, N. Hoyler, and J. Faist, *IEEE Photon. Technol. Lett.* **18**, 544 (2006).